Alpha and Theta EEG Rhythms Activity Reveal Deep Changes in Resting Brain State in Subjects with Prodromal Alzheimer's Disease

D.V. Moretti*, A. Prestia, G. Binetti, O. Zanetti and G.B. Frisoni

IRCCS S. Giovanni di Dio Fatebenefratelli, Brescia, Italy

Abstract: The increase of EEG alpha3/alpha2 frequency power ratio has been associated with AD-converters subjects with mild cognitive impairment (MCI) as well as a reduction in the regional cerebral blood flow (rCBF)

In this study, the association between alpha3/alpha2 frequency power ratio with rCBF changes in subjects with MCI was evaluated.

The alpha3/alpha2 frequency power ratio was computed in 27 subjects with MCI. Two groups were obtained according to the median values of alpha3/alpha2, at a cut-off of 1.17. In the groups so obtained, the correlation between brain perfusion and EEG markers were detected.

In the MCI group with the alpha3/alpha2 frequency power ratio above 1,17 as compared to the group with alpha3/alpha2 frequency power ratio below 1.17 there was: 1) a constant trend to lower rCBF values; 2) smaller hippocampal volumes; 3) higher theta frequency power.

The higher EEG alpha3 /alpha2 frequency power ratio individuates two different group of MCI subjects. A complex interplay between alpha and theta rhythms activity MCI patients is suggested in patients with prodromal Alzheimer's disease.

Keywords: EEG, alpha rhythm, theta rhythm, EEG, MCI, SPECT, resting state.

INTRODUCTION

In line with recently published research criteria [1, 2] it is becoming clear that a correct and early diagnosis of mild cognitive impairment (MCI) due to Alzheimer's disease (AD) is possible only with the integration of different biomarkers [1-3]. The most studied and validated biomarkers are markers of biological or morphostructural type. The Abeta42 and Tau protein in the cerebrospinal fluid (CSF), glucose metabolism on fluorodeoxyglucose positron emission tomography (18F-FDG PET), regional cerebral blood flow (rCBF) on single photon computed emission tomography (SPECT), atrophy of hippocampal volume (HV) on magnetic resonance imaging (MRI), and, more recently, brain amyloid deposition on amyloid imaging with PET [4, 5] are the most utilized biomarkers for the diagnosi of prodromal AD. Anyway, some weaknesses have been revealed as regards the actual biomarkers: 1) the lack a reliable specificity that allow a clear-cut diagnosis of the different subtypes of dementias; 2) thery are mainly based on the amiloid deposit theory, not universally accepted. So, there is the need of some new biomarkers, to integrate with the above mentioned criteria, in order to refine the early diagnosis of AD.

*Address correspondence to this author at the IRCCS 'San Giovanni di Dio – FBF', Via Pilastroni, 4 25125 Brescia, Italy; Tel: +39 0303501597; Fax: +39 0303533513; E-mail: davide.moretti@afar.it

The EEG could be a reliable tool for an early and highly predictive diagnosis of AD. It is widely accepted that the cerebral EEG rhythms reflect the underlying brain network activity [6-21]. An EEG marker was recently stated as an early sign of MCI due to AD, associated with altered structural and functional networks. Indeed, the increase of high alpha relative to low alpha frequency power is related to the hippocampal atrophy [14], to the amigdalo-hippocampal complex atrophy [16], as weel as to the conversion of patients with MCI in AD, but not in non-AD dementia [18-22]. The working hypothesis of the present study is that an increase in alpha3/alpha2 EEG frequency power ratio would like to be associated with lower brain perfusion in specific brain areas, as demonstrated in a large body of literature with SPECT studies [23-37]. Moreover, the relationship between functional and morphostructural markers are investigated to better understand the neurophysiological hallmarks of the early stage of AD.

METHODS

Subjects

MCI Patients

MCI patients were taken from a prospective project on MCI ("Mild Cognitive Impairment in Brescia – MCIBs"), aimed to study the natural history of persons without dementia with apparently primary cognitive

E-ISSN: 2309-6128/14

deficits, i.e. not due to psychic or physical conditions. The study protocol was approved by the local ethics committee and all participants signed an informed participation consent. Details on inclusion/exclusion criteria and on physical and neurological examinations, performance-based tests of physical function, gait and balance and performed neuropsychological battery have been previously published and are at disposable elsewhere [38]. Among the 56 MCI patients who agreed to undergo MRI and SPECT scan, all consecutive 27 who agreed also to undergo EEG recording were further considered.

Normal Controls

We enrolled all 17 healthy subjects from a previous study on cerebral perfusion correlates of conversion to AD with both an MRI and a SPECT scan available. Briefly, subjects were consecutive normal volunteers picked among those undergoing brain MRI scan at the Neuroradiology Unit of the "Città di Brescia"Hospital in Brescia from October 2004 to June 2006 for reasons unrelated to cognition, or were healthy volunteers aged 65 years or older, among MCI patients' spouses, friends of them, and researchers' acquaintances. All scans of enrolled subjects were normal on visual assessment of a neuroradiologist. Subjects underwent multidimensional assessment including clinical, neurological and neuropsychological evaluations, and drawing of a blood sample (not used for the purposes of the present study). Data coming from normal controls were used only to compute W scores in each selected perfusion ROI.

SPECT Scan

Both patients and normal controls underwent SPECT scan in the nuclear medicine department of the Ospedali Riuniti Hospital in Bergamo. Each patient received an intravenous injection of 925 MBq of technetium- 99m ethyl cysteinate dimer (^{99m}Tc-ECD) in resting conditions, lying supine with eyes closed in a quiet, dimly lit room. Forty to sixty minutes after injection, brain SPECT was performed using a dual-head rotating gamma camera (GE Elscint Helix) equipped with low energy-high resolution, parallel hole collimators. The advantage of dual head camera is a minor duration of the exam, a reduction of the rotational beam with a better spatial resolution, a reduction of the camera artifacts. A 128 x 128 pixel matrix, zoom=1.5, was used for image acquisition with 120 views over a 360° orbit (in 3° steps) with a pixel size and slice thickness of 2.94 mm. Butterworth filtered-back projection (order=7, cutoff= 0.45 cycles/cm) was used for image reconstruction, and attenuation correction was performed using Chang's method (attenuation coefficient=0.11 cm^{-1}). Images were exported in DICOM format. The best, sensitivity/specificity in distinguishing subjects with AD versus normal controls reached 96%/87%, by calculating a discriminant function based on regional cerebral blood flow (rCBF) of multiple brain regions. In early-stage AD, measurement of rCBF of the MTL results in sensitivity of 85%. This measurement improved to 96% for subjects with late-stage AD [39, 40].

SPECT Processing Protocol

To achieve a precise normalization, we generated a study-specific SPECT template using both SPECT and MRI scans of all patients and normal controls under study, following a procedure described in detail elsewhere [38]. Briefly, we created a customized high-definition MRI template, we converted SPECT scans to Analyze format using MRIcro [41], and we coregistered them to their respective MRI scans with SPM2 (SPM, Statistical Parametric Mapping, version 2 (2002). London: Functional Imaging Laboratory. Available at: http://www.fil.ion.ucl.ac.uk/spm/software/spm2). We normalized each MRI to the customized MRI template through a nonlinear transformation (cutoff 25mm), and we applied the normalization parameters to the coregistered SPECT. We obtained the customized SPECT template as the mean of all the latter normalized SPECT images. The creation of a study-specific template allows for better normalization, since low uptake in ventricular structures and cortical hypoperfusion effects are frequently present in elderly patients. For each coregistered SPECT scan, we set the origin to the anterior commissure, using the respective MRI image as a reference, and we processed all scans with SPM2 according to an optimized processing protocol described in detail elsewhere [38]. Brain perfusion correlates of medial temporal lobe atrophy and white matter hyperintensities in MCI were obtained as follows: (I) we smoothed each scan with a 10mm full width at half maximum (FWHM) Gaussian, and spatially normalized it with an affine deformation to the customized SPECT template; we applied the same deformation to the unsmoothed images; (II) we masked the unsmoothed normalized images from I to remove scalp activity using SPM2's "brainmask". We smoothed with a 10mm FWHM Gaussian, and warped them to the customized template with a nonlinear transformation (cutoff 25mm); we applied the same transformation to the unsmoothed masked images; (III) we smoothed the normalized unsmoothed images from II with a 12mm FWHM Gaussian. The following Region of Interest (ROI) were

chosen for perfusion analyses in each hemisphere from the Pick atlas by a sub-routine implemented on SPM2: frontal, parietal and temporal lobes, the thalamus and the hippocampal-amygdalar complex [42]. The choice of these regions was based on previous SPECT and PET studies in subjects with MCI [43-45].

The whole cerebellum was chosen for normalization of ROI counts. Since perfusion values in selected ROIs did not account for age, pertinent age corrected perfusion values (hereafter called W scores), were computed in each selected ROI, following a previously published procedure [46].

MR Imaging

Both patients and normal controls underwent brain T1-weighted magnetic resonance imaging in the neuroradiology department of the Città di Brescia Hospital, as previously discussed [38]. MR images were processed with SPM2 following an optimized Voxel- Based Morphometry protocol, described in detail elsewhere [32]. Manual tracings of hippocampal and total intracranial volumes were performed using DISPLAY (DISPLAY, Brain Imaging Center – Montreal Neurological Institute. Available at: http://www.bic.mni.mcgill.ca/software). Native hippocampal volumes were normalized to the individual intracranial volumes and rescaled to the mean total intracranial volume according to the following formula ([volume/individual total intracranial volume] *mean total intracranial volume). Total white matter lesions load was assessed trough visual Wahlund scale on T2 and FLAIR MRI images [47].

EEG Recordings

The EEG activity was recorded continuously from 19 sites by using electrodes set in an elastic cap (Electro-Cap International, Inc.) and positioned according to the 10–20 international systems (Fp1, Fp2, F7, F3, Fz, F4, F8, T3, C3, Cz, C4, T4, T5, P3, Pz, P4, T6, O1, and O2). The 19 electrodes array is the standard placement in the routine setting recordings. It has the advantage to be fast and easily reproducible allowing a ready comparison of the results among different studies. All recordings were obtained in the morning with subjects resting comfortably. In order to keep constant the level of vigilance, an operator controlled on-line the subject and the EEG traces, alerting the subject any time there were signs of behavioural and/or EEG drowsiness. The ground electrode was placed in front of Fz. The left and right mastoids served as reference for all electrodes. The recordings were used off-line to re-reference the scalp recordings to the common average. Re-referencing was done prior to the EEG artifact detection and analysis. Data were recorded with a band-pass filter of 0.3–70 Hz, and digitized at a sampling rate of 250 Hz (BrainAmp, BrainProducts, Germany). Electrodes-skin impedance was set below 5 khz. Horizontal and vertical eye movements were detected by recording the electrooculogram (EOG). The recording lasted 5 min, with subjects with closed eyes. Longer recordings would have reduced the variability of the data, but they would also have increased the possibility of slowing of EEG oscillations due to reduced vigilance and arousal. EEG data were then analyzed and fragmented off-line in consecutive epochs of 2 s, with a frequency resolution of 0.5 Hz. The average number of epochs analyzed was 140, ranging from 130 to 150. The EEG epochs with ocular, muscular and other types of artifact were preliminary identified by a computerized automatic procedure [9]. Two expert electroencephalographists manually double-checked and confirmed the automatic selections. The epochs with ocular, muscular and other types of artifacts were discarded.

Analysis of Individual Frequency Bands

A digital FFT-based power spectrum analysis (Welch technique, Hanning windowing function, no phase shift) computed – ranging from 2 to 45 Hz – the power density of EEG rhythms with a 0.5 Hz frequency resolution. Two anchor frequencies were selected according to the literature guidelines [48, 49], that is, the theta/alpha transition frequency (TF) and the individual alpha frequency (IAF) peak. These anchor frequencies were computed on the power spectra averaged across all recording electrodes. The TF marks the transition frequency between the theta and alpha bands, and represents an estimate of the frequency at which the theta and alpha spectra intersect. TF was computed as the minimum power in the alpha frequency range, since our EEG recordings were performed at rest. The IAF represents the frequency with the maximum power peak within the extended alpha range (5–14 Hz). Based on TF and IAF, we estimated the frequency band range for each subject, as follows: delta from TF-4 to TF- 2, theta from TF-2 to TF, low alpha band (alpha1 and alpha2) from TF to IAF, and high alpha band (or alpha3) from IAF to IAF + 2. The alpha1 and alpha2 bands were computed for each subject as follows: alpha1 from TF to the middle point of the TF-IAF range, and alpha2 from such middle point to the IAF peak [10-15]. Moreover, within theta frequency the frequency peak (individual theta frequency, ITF) was also individuated. The mean

frequency range computed in MCI subjects considered as a whole are: delta 2.9–4.9 Hz; theta 4.9–6.9 Hz; alpha1 6.9–8.9 Hz; alpha2 8.9–10.9 Hz; alpha3 10.9–12.9 Hz. Finally, in the frequency bands determined on an individual basis, we computed the relative power spectra for each subject. The relative power density for each frequency band was computed as the ratio between the absolute power and the mean power spectra from 2 to 45 Hz. The relative band power at each band was defined as the mean of the relative band power for each frequency bin within that band. The alpha3/alpha2 frequency power ratio was computed in all subjects. The 27 MCI patients enrolled for the present study with available MRI, SPECT and EEG recording were finally classified as at high risk (when the alpha3/alpha 2 EEG frequency power ratio median was above 1.17) or at low risk (when the alpha3/alpha 2 EEG frequency power ratio median was under 1.17) to develop AD. The choice of this cut-off was based on the median value, in order to balance the sample size of the two groups. Moreover, it was overlapping with the value we detected in previous studies, showing an high risk to develop AD in MCI subjects with the alpha3/alpha 2 EEG frequency power ratio above the value of 1.17 [9-15]. Of note, this cut-off individuates a MCI group with different pattern of both hippocampal atrophy, amigdalo-hippocampal complex atrophy and with a major risk to develops AD as compared to MCI group with alpha3/alpha2 EEG frequency power ratio values below 1.17 [16-22].

Statistical Analysis

All statistical analyses were performed using SPSS software ver. 13.0. We investigated significance of the difference between the 2 groups (MCI at low and at high risk to develop AD) in socio-demographic, clinical and cognitive features using χ^2 test for categorical variables (sex, and ApoE carriers) and Student's independent t test for continuous variables (volumetric, perfusion features and EEG frequencies). In all cases we set the significant threshold at $p<0.05$. Since native SPECT scans were coregistered to their respective MRI images, and the study-specific SPECT template was coregistered to the high-definition MRI template, all the normalized SPECT and MRI images used for the statistical analysis were coregistered to the SPM standard anatomical space. Moreover, Pearson's r correlations were assessed between the selected perfusion ROIs (in terms of age corrected W scores) and the acquired EEG frequencies in both groups.

RESULTS

27 MCI patients were enrolled for the present study and they were classified as at high risk (when the a3/a2 EEG rhythm median was above 1.17) or at low risk (when the a3/a2 EEG rhythm median was under 1.17) to develop AD. The two groups (AD high risk, N=13, AD low risk, N=14) were similar for age (p=0.56), education in years (p=0.87), gender (p=0.17), ApoE genotype (p=0.15), MMSE scores (p=0.31) and white matter lesions load (p=0.88; Table **1**). Figure **1** shows the visual rating scale of the SPECT scans representative of normal control, MCI with low and MCI with high risk to convert in AD, respectively. ANOVA results show that the selected cut-off was effective in detecting two different groups: patients with high risk to develop AD show significantly higher alpha3/alpha2 power ratio than patients with low risk (p=0.0001).

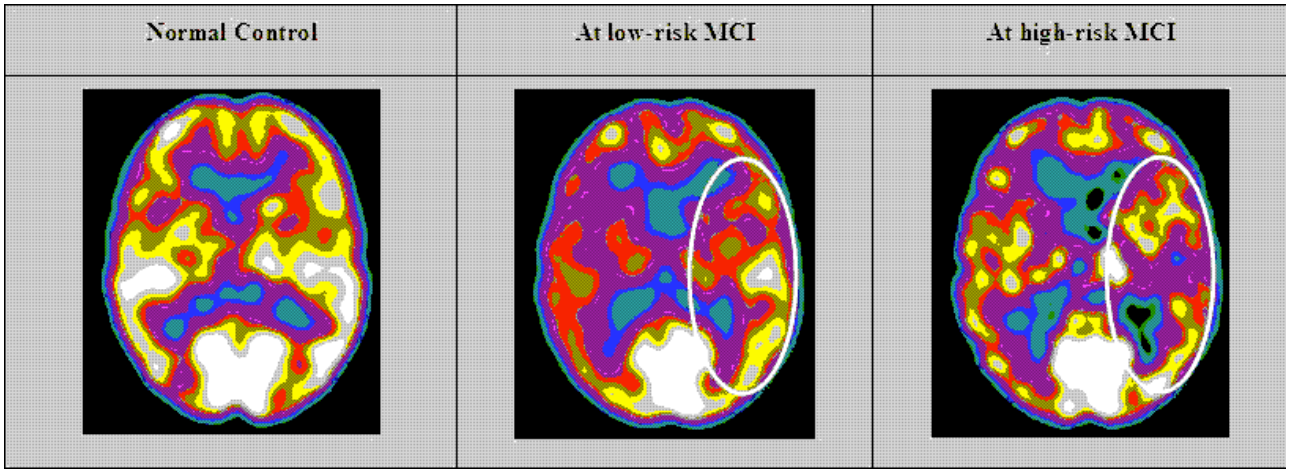

Figure 1: SPECT visual rating. The output shows a SPECT visual inspection of glucose uptake metabolism: the white square denotes an area of mild-to-moderate (purple to blue) temporparietal hypometabolism in one of the 14 at low risk and in one of the 13 at high risk MCI patient respect to one of the 17 enrolled controls

Moreover, a control analysis was performed on the single frequencies. The results show that the increase of alpha3/alpha2 frequency power ratio was due to both increase of alpha3 (p=0.001) and decrease of alpha 2 (p=0.0001) and not to the modification of a single frequency. This control analysis was performed because the change of only one frequency could be due to the chance. But it was not the case.

Table 1: Socio-Demographic, Clinical and Volumetric Features in MCI Patients by Risk to Develop AD. Values are Mean ± Standard Deviations for Continuous Variables or Frequency (percentage) for Gender and ApoE Carriers

	At low-risk MCI	At high-risk MCI	p
N	14	13	
Age (years) [Range]	69.1±7.6 [57÷83]	70.6±5.5 [62÷78]	0.555
Gender (females)	6 (43%)	9 (69%)	0.168
Education (years) [Range]	8.2±4.3 [4÷18]	7.9±4.5 [3÷18]	0.865
MMSE score [Range]	27.9±1.6 [25÷30]	27.2±1.9 [24÷29]	0.309
ApoE ε4 genotype (carriers)	2 (29%)	5 (39%)	0.152
Left Hippocampal Volume (mm^3) [Range]	2,606±353 [1,923÷3,017]	2,073±412 [1,234÷2,641]	0.001
Right Hippocampal Volume (mm^3) [Range]	2,581±473 [1,549÷3,150]	2,296±501 [1,589÷3,086]	141
Wahlund total score* [Range]	3.58±3.29 [0.0÷10.0]	3.78±2.63 [0.0÷7.0]	0.886

Table 2: Brain Perfusion and EEG Rhythms in MCI Patients by Risk to Develop AD. Values are Mean ± Standard Deviations. Brain Perfusion is Always Expressed as Age-Corrected Scores (W scores)

	At low-risk MCI	At high-risk MCI	p
N	14	13	
Frontal perfusion (W scores) [Range]	1.2±2.7 [-3.5÷5.5]	0.7±3.6 [-3.1÷11.8]	0.707
Parietal perfusion (W scores) [Range]	2.2±2.7 [-2.5÷7.0]	1.7±3.8 [-2.3÷13.3]	0.698
Temporal perfusion (W scores) [Range]	-4.9±2.5 [-8.9÷0.6]	-5.6±1.5 [-7.8÷-3.4]	0.384
Hippocampal Complex perfusion (W scores) [Range]	-2.3±2.0 [-6.5÷0.1]	-2.8±3.1 [-9.2÷0.6]	0.616
Thalamic perfusion (W scores) [Range]	-0.5±1.9 [-3.6÷4.9]	-0.6±1.4 [-3.4÷2.4]	0.860
EEG Alpha 1 [Range]	1.3±0.1 [1.1÷1.6]	1.4±0.1 [1.3÷1.5]	0.117
EEG Alpha 2 [Range]	3.6±0.3 [3.2÷4.1]	3.1±0.2 [2.7÷3.5]	0.0001
EEG Alpha 3 [Range]	3.7±0.2 [3.2÷4.0]	4.0±0.2 [3.7÷4.4]	0.001
EEG Alpha 3/Alpha2 [Range]	1.0±0.1 [0.9÷1.1]	1.3±0.1 [1.2÷1.5]	0.0001

Table 2 Continue ……

	At low-risk MCI	At high-risk MCI	p
EEG Beta 1 [Range]	0.5±0.2 [0.3÷1.0]	0.4±0.1 [0.2÷0.5]	0.175
EEG Beta 2 [Range]	0.4±0.1 [0.3÷0.7]	0.4±0.1 [0.2÷0.5]	0.393
EEG Theta [Range]	1.3±0.1 [1.2÷1.5]	1.3±0.1 [1.1÷1.6]	0.554
EEG Gamma [Range]	1.0±0.2 [0.6÷1.5]	0.8±0.2 [0.6÷1.2]	0.114
EEG Theta/Gamma [Range]	1.4±0.3 [0.8÷2.1]	1.6±0.5 [1.9÷2.9]	0.120

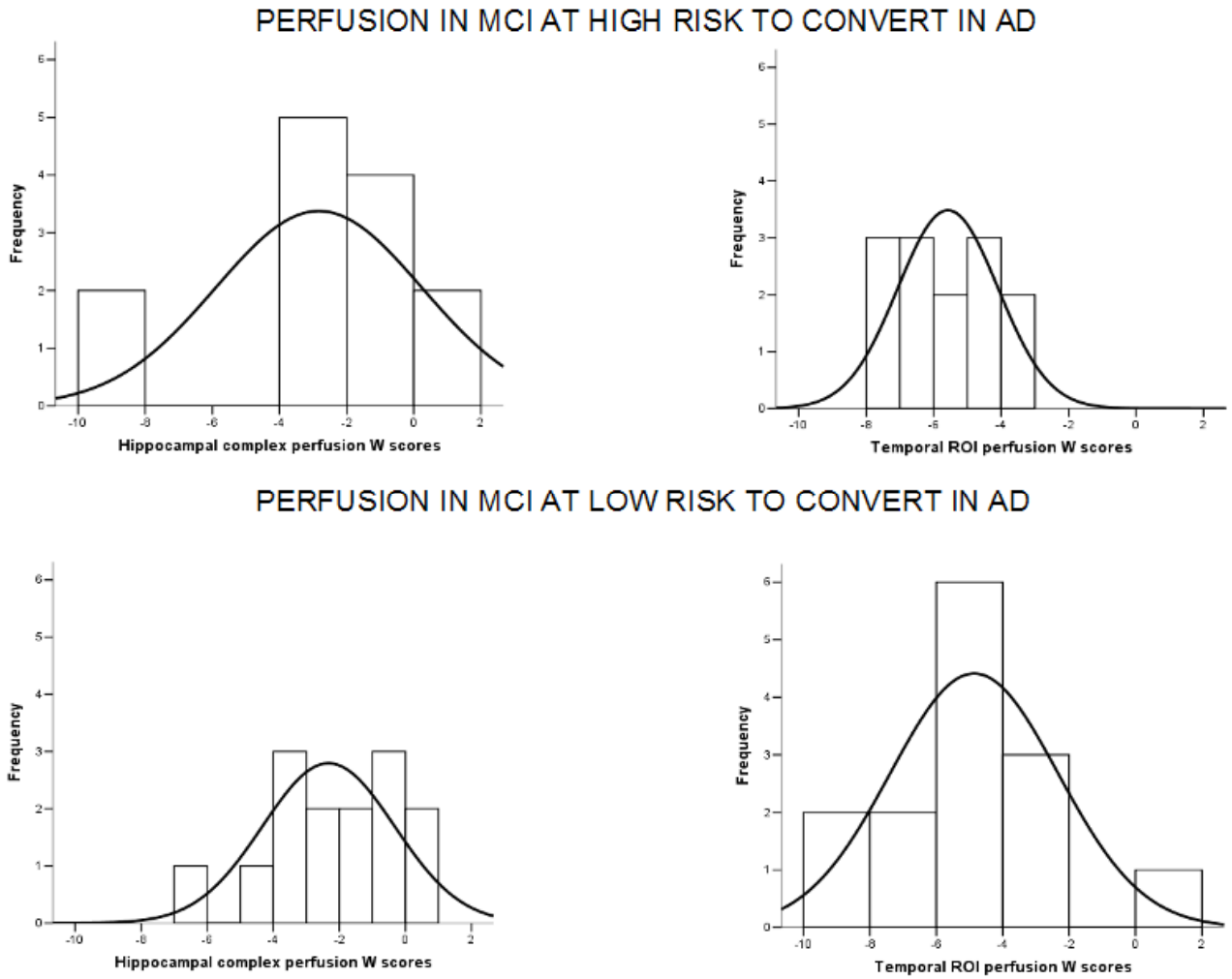

Figure 2: Histograms of the perfusion W scores distribution in at low and at high risk patients for hippocampal complex (left column) and temporal (right column) ROIs. Generally, for at high risk MCIs, perfusion scores are attested on lower values than at low risk patients. Black curve is the approximation to the normal distribution. X axis represents perfusion W scores while Y axis depicts the number of patients (frequency) for each W score.

Of note, no differences were found for beta 1, beta 2, gamma, theta EEG power and theta/gamma frequency power ratio (all p>0.11) (Table **2**). Although the mean perfusion in all the selected ROIs was similar between groups (all p>0.38), in the group with high alpha3/alpha2 frequency ratio there is a constant trend to a lower perfusion (see Figure **2**). Moreover, left hippocampal volumes were lower for AD-high risk patients respect to low risk ones (p=0.001) (Table **1**). Data coming from normal controls were used only to compute W scores in each selected perfusion ROI, but their summarized socio-demographic, clinical and volumetric features as well as their perfusion W scores can be found in Table **3**.

Table 3: Socio-Demographic, Clinical Volumetric and Brain Perfusion Features of Normal Elders Enrolled in the Study. Values are Mean ± Standard Deviations for Continuous Variables or Frequency (percentage) for Gender and ApoE Carriers. Brain Perfusion is always Expressed as Age-Corrected Scores (W scores)

	Normal controls
N	17
Age (years) [Range]	69.6±3.2 [65÷74]
Gender (females)	9 (53%)
Education (years) [Range]	9.8±4.1 [5÷19]
MMSE score [Range]	27.8±1.6 [24÷30]
ApoE ε4 genotype (carriers) *	1/12 (8%)
Left Hippocampal Volume (mm^3) [Range]	2,770±274 [2,089÷3,351]
Right Hippocampal Volume (mm^3) [Range]	2,715±221 [1,881÷3,139]
Frontal perfusion (W scores) [Range]	1.2±0.1 [1.1÷1.3]
Parietal perfusion (W scores) [Range]	1.4±0.1 [1.3÷1.5]
Temporal perfusion (W scores) [Range]	0.4±0.01 [0.4÷0.5]
Hippocampal Complex perfusion (W scores) [Range]	0.2±0.01 [0.18÷0.21]
Thalamic perfusion (W scores) [Range]	0.5±0.02 [0.49÷0.57]

* Missing data for 5 normal controls

In patients at low risk to develop AD, significant Pearson's R negative correlation was found between perfusion in the hippocampal complex ROI and theta rhythm (r=-0.544, p=0.044; Figure **3**).

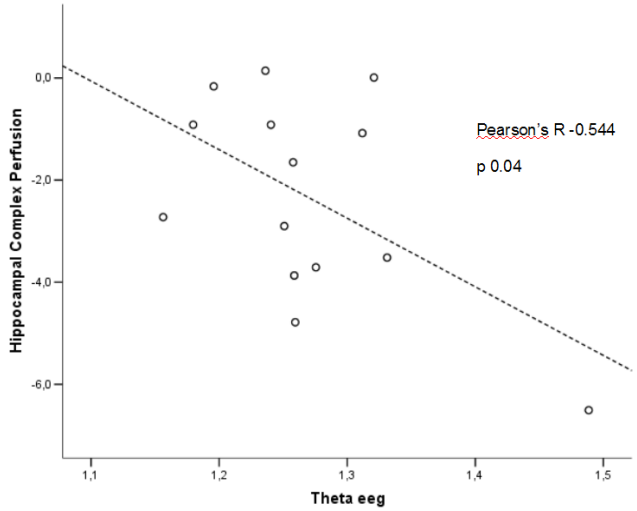

Figure 3: Pearson r correlations between EEG theta rhythm and hippocampal complex perfusion in patients at low risk to develop AD.

In patients at high risk to develop AD otherwise, more and dissimilar correlations were found: a positive correlation, inverted respect to patients at low risk, between the perfusion in the hippocampal complex ROI and theta rhythm (r=0.729, p=0.005; Figure **4**), while temporal ROI correlated positively with theta/gamma ratio rhythms (r=0.736, p=0.004; Figure **5**). No other significant correlations were found in both groups between perfusion ROIs and other EEG rhythms or hippocampal volumes. Moreover, no significant correlations were found between hippocampal complex ROI and theta rhythm pooling low and high risk patients together (r=0.086, p=0.671).

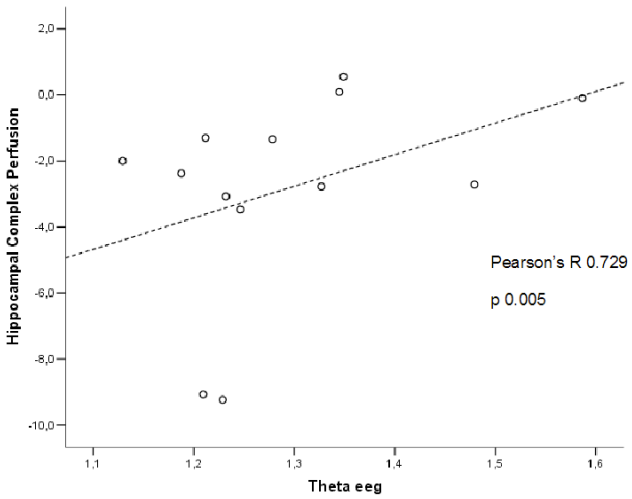

Figure 4: Pearson r correlations between EEG theta rhythm and hippocampal complex perfusion in patients at high risk to develop AD.

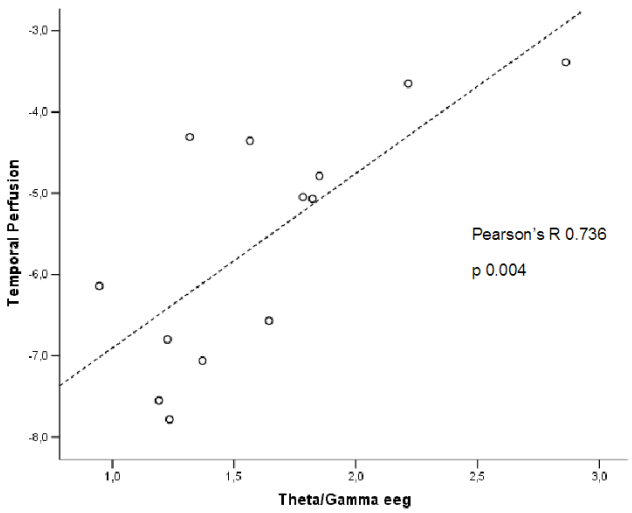

Figure 5: Pearson r correlations between EEG theta/gamma frequency ratio and temporal ROI perfusion in patients at high risk to develop AD.

DISCUSSION

The main aspect of the study is the correlation between cerebral perfusion and theta rhythm. Anyway, the correlation emerges only when considering the different groups individuated on the alpha3/alpha2 frequency power ratio. This is confirmed by the finding that when the groups are merged, no correlation could be found. The patients at lower risk to develop AD, who have a constant trend towards a higher brain regional blood perfusion, maintains low levels of hippocampal theta power while in patients at higher risk, with a basically lower cerebral blood perfusion, theta rhythm tends to be higher. A lot of studies have shown an increase of theta rhythm in patients with mild AD [50,51], so that the increase of theta power is a robust features of AD. Theta rhythms are thought to be produced by the activation of septal-hippocampal system. Hippocampus has a cholinergic innervation originating from basal forebrain, the medial septum, and the vertical limb of the diagonal band of Broca. Populations of GABAergic and glutamatergic neurons have also been described in several basal forebrain structures. The synchronized depolarization of hippocampal neurons produces field potentials that have a main frequency of 3–12 Hz and are usually known as hippocampal theta rhythm [52]. A cholinergic-glutamatergic hypothesis of AD, in which most symptoms may be explained by cholinergic-glutamatergic deficits, has been advanced. Neuronal injury/loss may include an excitotoxic component that possibly contributes to the early cholinergic deficit. This excitotoxic component may occur, at least in part, at the septal level where somas of cholinergic neurons are found. This insult may modify septal networks and contribute to the abnormal information processing observed in AD brain, including its hyperexcitability states. According to this theory, the increased theta production in AD would derive from hyperexcitability of the septal-hippocampal system [53]. Noteworthy, also a decrease in GABAergic input could provoke a loss of inhibition, arising the probability ot theta waves generation. A recent in vivo study ahs demonstrated the importance of N-methyl-d-aspartic acid (NMDA) glutamatergic stimulation to obtain theta oscillations [54].

On the other hand, cerebrovascular lesions should be considered as a possible cause of increase of theta rhythm. By means of observations in patients with ischemic lesions, it has been suggested that delays in corticocortical fiber propagation may play a global role in determining human EEG frequencies, increasing the amount of theta activity [55]. Increased T2 relaxation times in cortical gray matter and white matter were correlated with a shift in relative EEG power to lower frequencies in the theta range (4–7 Hz) and reduced cognitive performance [50]. Anyway, none of our patients suffered from acute ischemic lesions and there was no difference in the cerebrovascular load between the two groups. Moreover, the EEG frequency details of patients with chronic cerebrovascular load has been recently investigated [12] and they are not compatible with an high alpha3/alpha 2 frequency ratio increase. So, we are confident that our results are of neurodegenerative origin.

The alpha brain state has been related to psychological and physical well-being and with a mindfulness condition providing a full relaxation state [56]. On the other hand, the theta rhythm has been correlated to the enhancement of arousal and emotion, linked to limbic brain areas [57-58]. A possible interplay of theta and alpha EEG rhythms in MCI patients who will develop AD, could be related to the disruption of long-range, low alpha circuits (the mindfulness circuit), inducing the need of attention-related theta circuit, whose action provokes also an increase level of arousal and emotional behaviour. In this view, the increase of upper alpha/low alpha frequency ratio could be a window on the changes in the neural network assemblies of the prodromal AD, with encouraging prospective on the early diagnosis.

CONCLUSION

Our study reveals original and unknown aspects of a quite complex interplay between cerebral blood flow and electric activity dynamics and its association with hippocampal volume in a peculiar group of MCI patients, characterized by higher EEG alpha3 /alpha2 frequency ratio. The increase of upper alpha/low alpha ratio individuates a particular group of MCI subjects in which there is a reduction of the hippocampal volume and increase of theta rhythm activity and a reduction of the rCBF, all clinical features of prodromal AD. Moreover, in this study we have detected a precise cut-off revealing the MCI group at major risk to develop AD. The EEG alpha3/alpha2 frequency power ratio confirms a reliable neurophysiological marker powerful in clinical setting to make an early diagnosis of AD patients and helpful in research setting to validate the outcomes of drug clinical trials.

ACKNOWLEDGEMENTS

The work is funded by Fatebenefratelli Association for Research

DISCLOSURE STATEMENT

Moretti D V: I state that I have no actual or potential conflicts of interest.

Prestia A: I state that I have no actual or potential conflicts of interest.

Binetti G: I state that I have no actual or potential conflicts of interest.

Zanetti O: I state that I have no actual or potential conflicts of interest.

Frisoni G B: I state that I have no actual or potential conflicts of interest.

Moretti DV: on the behalf of all coauthors I declare that appropriate approval and procedures were used concerning human subjects

REFERENCES

[1] Albert MS, DeKosky ST, Dickson D, Dubois B, Feldman HH, Fox NC, Gamst A, Holtzman DM, Jagust WJ, Petersen RC, Snyder PJ, Carrillo MC, Thies B, Phelps CH. (2011). The diagnosis of mild cognitive impairment due to Alzheimer's disease: recommendations from the National Institute on Aging-Alzheimer's Association workgroups on diagnostic guidelines for Alzheimer's disease. Alzheimers Dement. 7(3):270-9. doi: 10.1016/j.jalz.2011.03.008.

[2] McKhann GM1, Knopman DS, Chertkow H, Hyman BT, Jack CR Jr, Kawas CH, Klunk WE, Koroshetz WJ, Manly JJ, Mayeux R, Mohs RC, Morris JC, Rossor MN, Scheltens P, Carrillo MC, Thies B, Weintraub S, Phelps CH. The diagnosis of dementia due to Alzheimer's disease: recommendations from the National Institute on Aging- Alzheimer's Association workgroups on diagnostic guidelines for Alzheimer's disease. Alzheimers Dement 2011;7:263–9. http://dx.doi.org/10.1016/j.jalz.2011.03.005

[3] Dubois B, Feldman HH, Jacova C, Dekosky ST, Barberger-Gateau P, Cummings J, Delacourte A, Galasko D, Gauthier S, Jicha G, Meguro K, O'brien J, Pasquier F, Robert P, Rossor M, Salloway S, Stern Y, Visser PJ, Scheltens P. (2007). Research criteria for the diagnosis of Alzheimer's disease: revising the NINCDS-ADRDA criteria. Lancet Neurol. Aug;6(8):734-46. Review.

[4] Hampel H, Bürger K, Teipel SJ, Bokde AL, Zetterberg H, Blennow K. (2008). Core candidate neurochemical and imaging biomarkers of Alzheimer's disease. Alzheimers Dement. 4:38–48. http://dx.doi.org/10.1016/j.jalz.2007.08.006

[5] Galluzzi S, Geroldi C, Amicucci G, Bocchio-Chiavetto L, Bonetti M, Bonvicini C, Cotelli M, Ghidoni R, Paghera B, Zanetti O, Frisoni GB; Translational Outpatient Memory Clinic Working. (2013). Supporting evidence for using biomarkers in the diagnosis of MCI due to AD Group. J Neurol. 260(2):640-50. doi: 10.1007/s00415-012-6694-0.

[6] Steriade M, Gloor P, LlinÃ s RR, Lopes da Silva FH, Mesulam M-M. (1990). Basic mechanisms of cerebral rhythmic activities. Eleciroenceph Clin Neurophysiol. 76:481-508. http://dx.doi.org/10.1016/0013-4694(90)90001-Z

[7] Steriade M. (2006). Grouping of brain rhythms in corticothalamic systems. Neuroscience. 137(4):1087-106. Review. http://dx.doi.org/10.1016/j.neuroscience.2005.10.029

[8] Missonnier P, Herrmann FR, Michon A, Fazio-Costa L, Gold G, Giannakopoulos P. (2010). Early disturbances of gamma band dynamics in mild cognitive impairment. J Neural Transm. Apr;117(4):489-98.

[9] Moretti DV, Babiloni F, Carducci F, Cincotti F, Remondini E, Rossini PM, Salinari S, Babiloni C. (2003). Computerized processing of EEG-EOG-EMG artifacts for multi-centric studies in EEG oscillations and event-related potentials. Int J Psychophysiol. 47(3):199-216. http://dx.doi.org/10.1016/S0167-8760(02)00153-8

[10] Moretti D.V., Babiloni C., Binetti G., Cassetta E., Dal Forno G., Ferreri F., Ferri R., Lanuzza B., Miniussi C., Nobili F., Rodriguez G., Salinari S., Rossini P.M. (2004). Individual analysis of EEG frequency and band power in mild Alzheimer's disease. Clin. Neurophysiol. 115, 299–308. http://dx.doi.org/10.1016/S1388-2457(03)00345-6

[11] Moretti D.V., Miniussi C. , Frisoni G., Zanetti O., Binetti G., Geroldi C., Galluzzi S., Rossini P.M. (2007). Vascular damage and EEG markers in subjects with mild cognitive impairment. Clinical neurophysiology. 118, 1866-1876. http://dx.doi.org/10.1016/j.clinph.2007.05.009

[12] Moretti D.V., Miniussi C., Frisoni G.B., Geroldi C., Zanetti O., Binetti G., Rossini P.M. (2007). Hippocampal atrophy and EEG markers in subjects with mild cognitive impairment. Clinical neurophysiology. 118, 2716-2729. http://dx.doi.org/10.1016/j.clinph.2007.09.059

[13] Moretti D.V., Frisoni G.B., Pievani M., Rosini S., Geroldi C., Binetti G., Rossini P.M. (2008). Cerebrovascular disease and hippocampal atrophy are differently linked to functional coupling of brain areas: an EEG coherence study in MCI subjects. J. Alzheimers. Dis. 14(3), 285-99.

[14] Moretti D.V., Pievani M., Fracassi C., Geroldi C., Calabria M., DeCarli C., Rossini P.M. (2008). Brain vascular damage of cholinergic pathways and E.E.G. markers in mild cognitive impairment. J. Alzheimers. Dis. 15(3), 357-72.

[15] Moretti D.V., Fracassi C., Pievani M., Geroldi C., Binetti G., Zanetti O., Sosta K., Rossini P. M. Frisoni G. B. (2009). Increase of theta/gamma ratio is associated with memory impairment. Clin. Neurophysiol. 120(2), 295-303. http://dx.doi.org/10.1016/j.clinph.2008.11.012

[16] Moretti D.V., Pievani M., Fracassi C., Binetti G., Rosini S., Geroldi C., Zanetti O., Rossini P.M., Frisoni G.B. (2009). Increase of theta/gamma and alpha3/alpha2 ratio is associated with amygdalo-hippocampal complex atrophy. J. Alzheimer Disease, 120 (2), 295-303.

[17] Moretti DV, Pievani M, Geroldi C, Binetti G, Zanetti O, Cotelli M, Rossini PM, Frisoni GB. (2009). Increasing hippocampal atrophy and cerebrovascular damage is differently associated with functional cortical coupling in MCI patients. Alzheimer Dis Assoc Disord. 23(4):323-32. http://dx.doi.org/10.1097/WAD.0b013e31819d4a9d

[18] Moretti DV, Frisoni GB, Fracassi C, Pievani M, Geroldi C, Binetti G, Rossini PM, Zanetti O. (2011). MCI patients' EEGs show group differences between those who progress and those who do not progress to AD. Neurobiology of aging. 32(4):563-71. http://dx.doi.org/10.1016/j.neurobiolaging.2009.04.003

[19] Moretti DV, Paternicò D, Binetti G, Zanetti O, Frisoni GB. (2012). EEG markers are associated to gray matter changes in thalamus and basal ganglia in subjects with mild cognitive impairment.Neuroimage. 60(1):489-96. http://dx.doi.org/10.1016/j.neuroimage.2011.11.086

[20] Moretti DV, Paternicò D, Binetti G, Zanetti O and Frisoni GB. (2013). Theta/Gamma Frequency Ratio is Associated to Grey Matter Changes in Basal Ganglia in Subjects with Mild Cognitive Impairment, Journal of Radiology and Diagnostic Imaging, 1, 10-18.

[21] Moretti DV, Paternico' D, Binetti G, Zanetti O and Frisoni GB. (2013). Relationship Between EEG Alpha3/Alpha2 Ration and the Nuclues Accumbens in Subjects with Mild Cognitive

Impairment. Journal of Neurology & Neurophysiology, 4,2; 1-6.

[22] Moretti DV, Paternico D, Binetti G, Zanetti O, Frisoni GB.EEG upper/low alpha frequency power ratio and the impulsive disorders network in subjects with mild cognitive impairment.Curr Alzheimer Res. 2014 Feb;11(2):192-9. http://dx.doi.org/10.2174/1567205011021403131555546

[23] Launes J, Sulkava R, Erkinjuntti T, Nikkinen P, Lindroth L, Liewendahl K, Iivanainen M. (1991). 99Tcm-HMPAO SPECT in suspected dementia. Nucl Med Commun. 12(9):757-65. http://dx.doi.org/10.1097/00006231-199109000-00002

[24] Mielke R, Pietrzyk U, Jacobs A, Fink GR, Ichimiya A, Kessler J, Herholz K, Heiss WD. (1994). HMPAO SPET and FDG PET in Alzheimer's disease and vascular dementia: comparison of perfusion and metabolic pattern. Eur J Nucl Med. 21(10):1052-60. http://dx.doi.org/10.1007/BF00181059

[25] Minoshima S, Foster NL, Kuhl DE. (1994). Posterior cingulate cortex in Alzheimer's disease. Lancet 344:895. http://dx.doi.org/10.1016/S0140-6736(94)92871-1

[26] Rodriguez G, Nobili F, Copello F, Vitali P, Gianelli MV, Taddei G, Catsafados E, Mariani G. (1999). 99mTc-HMPAO regional cerebral blood flow and quantitative electroencephalography in Alzheimer's disease: a correlative study. J Nucl Med. Apr;40(4):522-9.

[27] Rodriguez G, Vitali P, Canfora M, Calvini P, Girtler N, De Leo C, Piccardo A, Nobili F. (2004). Quantitative EEG and perfusional single photon emission computed tomography correlation during long-term donepezil therapy in Alzheimer's disease. Clin Neurophysiol. 115(1):39-49. http://dx.doi.org/10.1016/S1388-2457(03)00321-3

[28] Kogure D, Matsuda H, Ohnishi T, Asada T, Uno M, Kunihiro T, Nakano S, Takasaki M. (2000). Longitudinal evaluation of early Alzheimer's disease using brain perfusion SPECT. J Nucl Med 41:1155Y1162.

[29] Jagust W, Thisted R, Devous MD Sr, Van Heertum R, Mayberg H, Jobst K, Smith AD, Borys N. (2001). SPECT perfusion imaging in the diagnosis of Alzheimer's disease: a clinical-pathologic study. Neurology. 56:950–6. http://dx.doi.org/10.1212/WNL.56.7.950

[30] Forlenza OV, Diniz BS, Gattaz WF. (2010). Diagnosis and biomarkers of predementia in Alzheimer's disease. BMC Med. 22;8:89. doi: 10.1186/1741-7015-8-89.

[31] Frisoni GB, Scheltens Ph, Galluzzi S, Nobili FM, Fox NC, Robert PH, Soininen H, Wahlund LO, Waldemar G, Salmon E. (2003). Neuroimaging tools to rate regional atrophy, subcortical cerebrovascular disease, and regional cerebral blood flow and metabolism: consensus paper of the EADC. J Neurol Neurosurg Psychiatry. 74(10):1371-81. http://dx.doi.org/10.1136/jnnp.74.10.1371

[32] Frisoni GB, Testa C, Sabattoli F, Beltramello A, Soininen H, Laakso MP. (2005). Structural correlates of early and late onset Alzheimer's disease: voxel based morphometric study.; J Neurol Neurosurg Psychiatry 76: 112–114. http://dx.doi.org/10.1136/jnnp.2003.029876

[33] Frisoni GB. (2012). Alzheimer disease: Biomarker trajectories across stages of Alzheimer disease. Nat Rev Neurol. 8;8(6):299-300. doi: 10.1038/nrneurol.2012.81.

[34] Golde TE. (2003). Alzheimer disease therapy: Can the amyloid cascade be halted? J Clin Invest. 111:11-18. http://dx.doi.org/10.1172/JCI200317527

[35] Gungor HA, Yildiz A, Aydin F, Gungor F, Boz A, Ozkaynak S. (2005). Tc-99m HMPAO brain SPECT findings in mild and moderate Alzheimer's disease: correlation with event related potentials. J Neurol Sci. 15;234(1-2):47-53.

[36] Pupi A, Mosconi L, Nobili FM, Sorbi S. (2005). Toward the validation of functional neuroimaging as a potential biomarker for Alzheimer's disease: implications for drug development. Mol Imaging Biol. Jan-Feb;7(1):59-68.

[37] Nobili F, De Carli F, Frisoni GB, Portet F, Verhey F, Rodriguez G, Caroli A, Touchon J, Morbelli S, Guerra UP, Dessi B, Brugnolo A, Visser PJ. (2009). SPECT predictors of cognitive decline and Alzheimer's disease in mild cognitive impairment. J Alzheimers Dis. 17(4):761-72. doi: 10.3233/JAD-2009-1091.

[38] Caroli A, Testa C, Geroldi C, Nobili F, Guerra UP, Bonetti M, Frisoni GB. (2007). Brain perfusion correlates of medial temporal lobe atrophy and white matter hyperintensities in mild cognitive impairment. J Neurol. Aug;254(8):1000-8.

[39] Tsolaki M, Sakka V, Gerasimou G, Dimacopoulos N, Chatzizisi O, Fountoulakis KN, Kyriazis G, Papanastasiou J, Kazis A. Correlation of rCBF (SPECT), CSF tau, and cognitive function in patients with dementia of the Alzheimer's type, other types of dementia, and control subjects. Am J Alzheimers Dis Other Demen. 2001; 16(1):21-31. http://dx.doi.org/10.1177/153331750101600107

[40] Wollman D E., Prohovnik I. Sensitivity and specificity of neuroimaging for the diagnosis of Alzheimer's diseaseDialogues Clin Neurosci. 2003;5:89-99.

[41] Rorden C, Brett M (2000): Stereotaxic display of brain lesions. Behav Neurol 12:191–200. http://dx.doi.org/10.1155/2000/421719

[42] Maldjian JA, Laurienti PJ, Kraft RA, Burdette JH. (2003). An Automated Method for Neuroanatomic and Cytoarchitectonic Atlas-based Interrogation of fMRI Data Sets. Neuroimage 19, 1233-1239. http://dx.doi.org/10.1016/S1053-8119(03)00169-1

[43] Staffen W, Bergmann J, Schönauer U, Zauner H, Kronbichler M, Golaszewski S, Ladurner G. (2009). Cerebral perfusion (HMPAO-SPECT) in patients with depression with cognitive impairment versus those with mild cognitive impairment and dementia of Alzheimer's type: a semiquantitative and automated evaluation. Eur J Nucl Med Mol Imaging. 36(5):801-10. http://dx.doi.org/10.1007/s00259-008-1028-2

[44] Yoon HJ, Park KW, Jeong YJ, Kang DY. (2012). Correlation between neuropsychological tests and hypoperfusion in MCI patients: anatomical labeling using xjView and Talairach Daemon software. Ann Nucl Med. Oct;26(8):656-64.

[45] Alegret M, Cuberas-Borrós G, Vinyes-Junqué G, Espinosa A, Valero S, Hernández I, Roca I, Ruíz A, Rosende-Roca M, Mauleón A, Becker JT, Castell-Conesa J, Tárraga L, Boada M. (2012). A two-year follow-up of cognitive deficits and brain perfusion in mild cognitive impairment and mild Alzheimer's disease. J Alzheimers Dis. 30(1):109-20.

[46] Jack CR Jr, Petersen RC, Xu YC, Waring SC, O'Brien PC, Tangalos EG, Smith GE, Ivnik RJ, Kokmen E. (1997). Medial temporal atrophy on MRI in normal aging and very mild Alzheimer's disease. Neurology; 49:786–94. http://dx.doi.org/10.1212/WNL.49.3.786

[47] Wahlund LO, Barkhof F, Fazekas F, Bronge L, Augustin M, Sjögren M, Wallin A, Ader H, Leys D, Pantoni L, Pasquier F, Erkinjuntti T, Scheltens P. (2001). European Task Force on Age-Related White Matter Changes. A new rating scale for age-related white matter changes applicable to MRI and CT. Stroke. 32(6):1318-22. http://dx.doi.org/10.1161/01.STR.32.6.1318

[48] Klimesch W. (1997). EEG-alpha rhythms and memory processes, Int J Psychophysiol. 26: 319– 340. http://dx.doi.org/10.1016/S0167-8760(97)00773-3

[49] Klimesch W. (1999). EEG alpha and theta oscillations reflect cognitive and memory performance: a review and analysis. Brain Res Rev. 29: 169–95. http://dx.doi.org/10.1016/S0165-0173(98)00056-3

[50] Rodriguez G, Arnaldi D, Picco A. (2011). Brain functional network in Alzheimer's disease: diagnostic markers for diagnosis and monitoring. Int J Alzheimers Dis. doi: 10.4061/2011/481903

[51] Rodriguez G, Vitali P, Calvini P, Bordoni C, Girtler N, Taddei G, Mariani G, Nobili F. (2000). Hippocampal perfusion in mild Alzheimer's disease. Psychiatry Res. 4;100(2):65-74.

[52] Bland BH and Colom LV. (1993). "Extrinsic and intrinsic properties underlying oscillation and synchrony in limbic cortex," Progress in Neurobiology, vol. 41, no. 2, pp. 157–208. http://dx.doi.org/10.1016/0301-0082(93)90007-F

[53] Colom LV. (2006). Septal networks: relevance to theta rhythm, epilepsy and Alzheimer's disease. Journal of Neurochemistry, vol. 96, no. 3, pp. 609–623. http://dx.doi.org/10.1111/j.1471-4159.2005.03630.x

[54] Kazmierska P1, Konopacki J. Development of NMDA-induced theta rhythm in hippocampal formation slices. Brain Res Bull. 2013 Sep;98:93-101. doi: 10.1016/j.brainresbull.2013.07.010. Epub 2013 Jul 26. http://dx.doi.org/10.1016/j.brainresbull.2013.07.010

[55] Thatcher RW, Biver C, McAlaster R, and Salazar A. (1998). Biophysical linkage between MRI and EEG coherence in closed head injury. NeuroImage, vol. 8, no. 4, pp. 307–326. http://dx.doi.org/10.1006/nimg.1998.0365

[56] Stinson B, Arthur D. A novel EEG for alpha brain state training, neurobiofeedback and behavior change. Complement Ther Clin Pract. 2013 Aug;19(3):114-8. doi: 10.1016/j.ctcp.2013.03.003. Epub 2013 Apr 19.

[57] Müller TJ, Thome J, Chiaramonti R, Dierks T, Maurer K, Fallgatter AJ, Frölich L, Scheubeck M, Strik WK. (1997). A comparison of qEEG and HMPAO-SPECT in relation to the clinical severity of Alzheimer's disease. Eur Arch Psychiatry Clin Neurosci. 247(5):259-63. http://dx.doi.org/10.1007/BF02900304

[58] Gruzelier J. A theory of alpha/theta neurofeedback, creative performance enhancement, long distance functional connectivity and psychological integration. Cogn Process. 2009 Feb;10 Suppl 1:S101-9. doi: 10.1007/s10339-008-0248-5.

Received on 19-03-2014 Accepted on 24-03-2014 Published on 04-09-2014

DOI: http://dx.doi.org/10.12974/2309-6128.2014.02.01.3